

3.3 Strongly Correlated Quantum Systems

Machine learning and *ab initio* analyses of cuprate high-temperature superconductors

Masatoshi IMADA

Toyota Physical and Chemical Research Institute

41-1 Yokomichi, Nagakute, Aichi, 480-1192

and

Research Institute for Science and Engineering, Waseda University

3-4-1 Okubo, Shinjuku-ku, Tokyo, 169-8555

Understanding physics of high- T_c cuprate superconductors remains one of the challenges in physics. In this project, we have continued efforts to clarify physics and mechanism of high-temperature superconductivity, particularly for the copper oxides. This is a combined research activity of three different approaches:

- (1) Parameter search of strongly correlated electron models by using high-accuracy solvers for quantum many-body lattice Hamiltonians
- (2) Parameter-free *ab initio* studies of real materials by using multi-scale *ab initio* scheme for correlated electrons (MACE) [1]
- (3) Data science approaches to expose hidden physical quantities and mechanisms by combining extended experimental data such as by angle resolved photoemission spectroscopy (ARPES), quasiparticle interference (QPI) by scanning tunnel microscope (STM) and resonant inelastic X-ray scattering (RIXS) with the help of applied mathematical and information science technology such as machine-learning tools.

In the first approach, we have continued to clarify physics of electron fractionalization and formation of topological states such as quantum

spin liquids (QSL). It was achieved by using the variational Monte Carlo tools (mVMC) [2] combined with the restricted Boltzmann machine developed by us [3,4], tensor network [5,6] and the Lanczos diagonalization. In the J_1J_2 Heisenberg model defined on the 2D square lattice with the nearest neighbor exchange interaction (J_1) and the next nearest neighbor exchange (J_2), we have further firmly established the existence of the QSL in the region $0.49 < J_2/J_1 < 0.54$ [7]. The analyses were elaborated by comparing the accuracy of our solver with other tools in the literature. The accuracy and reliability of our solver were shown to be the best among existing solvers both for the ground states and the excitations. The reliability and robustness of the analyses was confirmed by (i) the size insensitivity of the correlation-ratio crossing points to identify the QSL-antiferromagnetic transition and the QSL to valence-bond-solid transition (ii) the insensitivity about the choice of the initial variational parameters for the wavefunction (iii) better size extrapolation of the level crossing point to infer the ground state phase boundary

from the level crossing points of the excitation spectra, where larger size calculation has been added to enhance the accuracy of the extrapolation.

We have also been investigating the quantum ground state of the $S=1/2$ Heisenberg antiferromagnet on the pyrochlore lattice [8]. After investigation of various trial wave functions, we find that the singlet ground state has a linear dispersion at vanishing momentum with a finite energy gap to triplet excitations. Furthermore, it has turned out that the ground state is fully degenerate for all the point group symmetry represented by the irreducible symmetry group, which implies an emergence of the unprecedented type of quantum spin liquid.

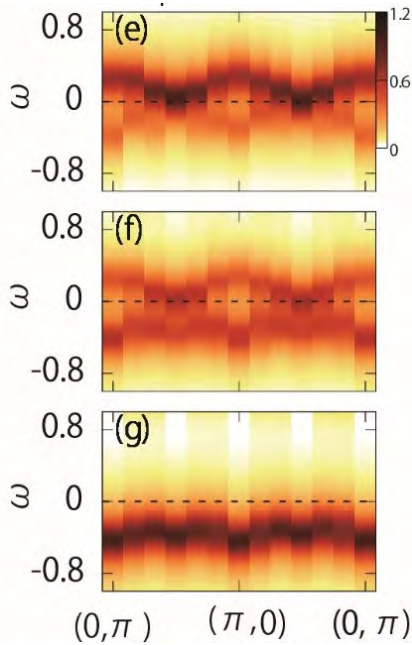


Fig.1: Spectral function along around symmetry line. (f) is closest to the symmetry line showing a large d -wave gap at $(\pi,0)$ [10].

Accurate algorithms and tools for quantum dynamics were also sought for [9]. A method to calculate spectral functions measurable by the ARPES representing the imaginary part of the electron single-particle Green's function was developed in addition to the two-particle dynamical structure factor for spin and charge [10]. The application to the Hubbard model revealed the d -wave gap structure for the first time in the superconducting state as shown in Fig.1. It has shown an unrealistically large gap of the typical Hubbard model implying an oversimplified nature of the Hubbard model as a model of the cuprate superconductors.

For the *ab initio* approaches (2), we have reproduced the experimental phase diagram of $\text{HgBa}_2\text{CuO}_{4+y}$ [11] by solving its *ab initio* low-energy effective Hamiltonian without adjustable parameters [12]. Thanks to this success, in the present project in 2020, more thorough and systematic analyses for several different copper oxide compounds have started. Derivation of *ab initio* low-energy effective Hamiltonians for the series of multi-layer compounds including Bi and solving with refined mVMC tool is under way.

The third data science approach (3) has been elaborated for the machine learning analysis of the ARPES data. The comparison with the literature has clarified the reliability of our analyses, which shows the emergence of prominent peak structures in the normal and anomalous parts of the self-energies and their

cancellation in the Green's function resulting in the direct invisibility in ARPES, while the prominent peak is the origin of the high temperature superconductivity [13]. The accuracy and reliability of the present machine learning method were confirmed by several benchmark tests, which successfully reproduced the expected exact results and the established analyses in the literature. It further established the robustness against unavoidable experimental noise and extrinsic contributions to spectral functions such as background effects. The origin of the failure of previous studies which did not find the prominent structure in the self-energies are exposed by faithfully following the assumptions by the previous studies and by showing the error contained in the assumptions.

More thorough studies of the integrated spectroscopy analysis have been conducted in the combination of ARPES, and QPI or RIXS. By using the ARPES data and their machine learning analyses, a two-component fermion model is constructed to represent the fractionalization of electrons supported by the previous theoretical and experimental studies. Then the two-component Hamiltonian was analyzed to predict the RIXS data [14]. The prediction shows a substantial enhancement of the RIXS intensity in the superconducting phase in comparison to the normal phase, if the electron fractionalization correctly describes the low energy dynamics of the cuprate superconductors. Since such an enhancement

does not occur in the absence of the fractionalization, it can be used as the stringent test for the occurrence of the fractionalization.

This is a combined report for E project 2020-Ea-0005 and 2020-Eb-0005 as well as shared project for Fugaku project.

This series of work has been done in collaboration with T. Misawa, M. Hirayama, K. Ido, Y. Nomura, Y. Yamaji, R. Pohle, M. Charlebois, J-B. Moree, F. Imoto, A. Fujimori and T. Yoshida. The work is also supported by JSPS Kakenhi 16H06345, the RIKEN Center for Computational Science under the HPCI project (hp200132) This project has used the software HPhi, mVMC and RESPACK.

References

- [1] M. Imada and T. Miyake: J. Phys. Soc. Jpn. **79** (2010) 112001
- [2] T. Misawa *et al.*: Comput. Phys. Commun. **235** (2019) 447
- [3] Y. Nomura *et al.*: Phys. Rev. B.96 (2017) 205152
- [4] G. Carleo *et al.*: Nat. Commun. 9 (2018) 5322
- [5] H.-H. Zhao *et al.*: Phys. Rev. B.96 (2017) 085103
- [6] A. S. Darmawan *et al.*: Phys. Rev. B 98 (2018) 205132.
- [7] Y. Nomura and M. Imada: arXiv:2005.14142.
- [8] R. Pohle, Y. Yamaji and M. Imada: unpublished.
- [9] M. Charlebois and M. Imada: Phys. Rev. X 10 (2020) 041023.
- [10] K. Ido, M. Imada and T. Misawa: Phys. Rev. B 101 (2020) 075124
- [11] T. Ohgoe *et al.*, Phys. Rev. B **101** (2020) 045124.
- [12] M. Hirayama *et al.*: Phys. Rev. B **99** (2019) 245155.
- [13] Y. Yamaji *et al.*: arXiv:1903.08060
- [14] M. Imada, arXiv:2103.10016.

Numerical studies of quantum spin liquids by quantum mutual information

Youhei YAMAJI

GREEN, National Institute for Materials Science

Namiki, Tsukuba-shi, Ibaraki, 305-0044

Recent studies on quantum spin liquids (QSLs) revealed that a wide variety of the QSLs is characterized by emergent fractionalized excitations and their topological nature, instead of an absence of spontaneous symmetry breaking at zero temperature. Entanglement entropy has been proposed to distinguish topologically trivial and non-trivial states. Although the entanglement entropy is hard to measure in experiments, it is applicable to any many-body states.

Instead of the entanglement entropy, mutual information (MI), a generalization of entanglement entropy, is useful at finite temperatures, where temperature scales characterizing the fractionalization may emerge. The MI is given as relative entropy between the density matrix and a product of reduced density matrices of a given system: When the system is divided into two subsystems, X and Y , the MI I is given as $I = \text{tr} [\hat{\rho} \{ \ln \hat{\rho} - \ln(\hat{\rho}^X \otimes \hat{\rho}^Y) \}]$, where $\hat{\rho}$ is the density matrix and $\hat{\rho}^X$ ($\hat{\rho}^Y$) is the reduced density matrix for the subsystem X (Y) by taking a partial trace over the complementary subsystem Y (X).

Naively, the computational and memory costs for I are higher than those for obtaining an eigenstate. However, typical state approaches enable us to estimate I with $\mathcal{O}(N_H)$ computational and memory costs, where N_H is the Hilbert space dimension of the target system, although the density matrix consisting of a typical pure state shows unphysical properties, as follows. When one define

the density matrix with a canonical thermal pure quantum (cTPQ) state [1, 2] as, $\hat{\rho}_{\text{pure}} = |\Phi(\beta)\rangle\langle\Phi(\beta)| / \langle\Phi(\beta)|\Phi(\beta)\rangle$, where $|\Phi(\beta)\rangle = e^{-\beta\hat{H}/2}|\Phi(0)\rangle$ and $|\Phi(0)\rangle$ is a normalized random vector. As emphasized in the literature, $\hat{\rho}_{\text{pure}}$ is different from $\hat{\rho}$: any integer power of $\hat{\rho}_{\text{pure}}$ is equal to $\hat{\rho}$ as $\mathbb{E}[\hat{\rho}_{\text{pure}}^m] = \hat{\rho}$, where \mathbb{E} is the average over distribution of the random vector $|\Phi(0)\rangle$ and $Z(\beta) = \sum_n e^{-\beta E_n}$. In contrast, the reduced density matrix constructed from $\hat{\rho}_{\text{pure}}$ for the subsystem X (Y), $\hat{\rho}_{\text{pure}}^X$ ($\hat{\rho}_{\text{pure}}^Y$), satisfies $\hat{\rho}^{X/Y} = \mathbb{E}[\hat{\rho}_{\text{pure}}^{X/Y}]$.

Because $\hat{\rho}_{\text{pure}}^{X/Y}$ and $\hat{\rho} \ln \hat{\rho} = -S(\beta)$, where $S(\beta)$ is entropy at inverse temperatures β , are calculated by the cTPQ with $\mathcal{O}(N_H)$ computational and memory costs, $\hat{\rho} \ln(\hat{\rho}^X \otimes \hat{\rho}^Y)$ can be calculated with the similar costs. Here, we note that $\hat{\rho}$ appears only once in $\hat{\rho} \ln(\hat{\rho}^X \otimes \hat{\rho}^Y)$. The MI of an *ab initio* hamiltonian for Na_2IrO_3 has been simulated and the temperature dependence will be published. The reduced density matrices are also useful to clarify the nature of correlated electrons such as high-temperature superconductivity [3].

References

- [1] S.Lloyd: arXiv:1307.0378; Ph.D. Thesis, Rockefeller University (1988)
- [2] S. Sugiura and A. Shimizu: Phys. Rev. Lett. **111** (2012) 010401.
- [3] A. Iwano: master's thesis, The University of Tokyo (2020).

Numerical studies of quantum spin liquid candidates by highly accurate *ab initio* effective hamiltonians

Youhei YAMAJI

GREEN, National Institute for Materials Science

Namiki, Tsukuba-shi, Ibaraki, 305-0044

A Kitaev's spin liquid candidate, α - RuCl_3 , has attracted considerable attention. Although several studies on the effective hamiltonian of α - RuCl_3 , there is no consensus on the effective hamiltonian and no effective hamiltonian consistently explains experimentally observed specific heat and inelastic neutron scatterings. While these effective hamiltonians significantly deviate from the Kitaev model, the ruthenium halide shows experimental signatures of Majorana excitations. To refine the effective hamiltonian of the ruthenium halide and to clarify whether the ruthenium halide is in the vicinity of the Kitaev model or not, we theoretically study the series of the ruthenium halides, α - RuH_3 ($H=\text{Cl, Br, I}$).

Recent developments of deriving *abinitio* effective hamiltonians by using localized Wannier orbitals and constrained random phase or *GW* approximations [1, 2] enables us to study spin-orbit coupled Mott insulators and correlated (semi)metals. Regardless of the details of these methods, as the ionic radius of the halogen atom increases from Cl to I, the correlations in the ruthenium halides become weaker. The detailed analyses on the effective *abinitio* spin hamiltonians and itinerant electron hamiltonians are performed by using $\mathcal{H}\Phi$ [3] and mVMC [4]. The spin hamiltonian seems to be invalid for $H = \text{I}$ and, at least, t_{2g} hamiltonians are required to describe the end member of the ruthenium halides.

To characterize the excitation spectra of correlated electrons, we have also developed nu-

merical procedures to simulate *abinitio* spectral functions for the many-body Schrödinger equation, instead of the effective lattice hamiltonians, by combining variational Monte Carlo methods and Krylov subspace methods [5]. To examine the applicability of the present algorithm, it is applied to the single particle spectral functions of liquid helium 3. The self-energy is derived, which explicitly demonstrate the strongly correlated nature of liquid helium 3 in an *abinitio* fashion.

References

- [1] M. Charlebois, J.-B. Morée, K. Nakamura, Y. Nomura, T. Tadano, Y. Yoshimoto, Y. Yamaji, T. Hasegawa, K. Matsuhira, M. Imada: arXiv:2103.09539.
- [2] J.-B. Morée, S. Biermann, Y. Yamaji, and M. Imada: unpublished.
- [3] M. Kawamura, K. Yoshimi, T. Misawa, Y. Yamaji, S. Todo, and N. Kawashima: *Compt. Phys. Communi.* **217** (2017) 180.
- [4] T. Misawa, S. Morita, K. Yoshimi, M. Kawamura, Y. Motoyama, K. Ido, T. Ohgoe, M. Imada, and T. Kato: *Compt. Phys. Communi.* **235** (2019) 447.
- [5] N. Okada: *Dynamical Variational Monte Carlo Approaches for Excitation Spectra of Many-Body Fermions in Continuum Space*, master's thesis, The University of Tokyo (2020).

Systematic analysis of *ab initio* low-energy effective Hamiltonians for Pd(dmit)₂ molecular conductors

Takahiro Misawa

*Institute for Solid State Physics, University of Tokyo
Kashiwa-no-ha, Kashiwa, Chiba 277-8581*

Quantum spin liquids, which do not show any symmetry breaking even at zero temperature, have attracted much interest since their elementary excitations in the quantum spin liquids are expected to show exotic elementary excitations such as Majorana particles. Because the exotic elementary excitations may be useful for next-generation devices such as quantum computers, a huge amount of works on searching and identifying the quantum spin liquids in solids has been done in a decade.

Among several candidates of the quantum spin liquids, the molecular solids β' - $X[\text{Pd}(\text{dmit})_2]_2$ (X represents a cation) offers an ideal platform for realizing the quantum spin liquid induced by the geometrical frustration in the magnetic interactions because the geometrical frustration can be systematically controlled by changing cations X . In experiments, it has been proposed that the Neel temperatures are systematically controlled by changing cations X and the quantum spin liquid realizes in $X = \text{EtMe}_3\text{Sb}$ [1, 2].

In this project, to identify the microscopic origin of the quantum spin liquid found in $X = \text{EtMe}_3\text{Sb}$, we have performed systematic and comprehensive *ab initio* derivations of low-energy effective Hamiltonians for available 9 compounds of β' - $X[\text{Pd}(\text{dmit})_2]_2$ ($X = \text{Me}_4\text{Y}$, EtMe_3Y , $\text{Et}_2\text{Me}_2\text{Y}$ and $\text{Y} = \text{As}$, Sb , and P) [3]. In the derivation the low-energy effective Hamiltonians, we first obtain the global band structure for dmit-salts using Quantum ESPRESSO [4]. Then, using the open-source

software package RESPACK [5, 6], we evaluate the transfer integrals and two-body interactions such as the Coulomb interactions. As a result, we have found that the anisotropy of the transfer integrals and correlations effects systematically change by changing cations.

Moreover, we have analyzed the low-energy effective Hamiltonians using the exact diagonalization method [7, 8]. From the numerical exact analyzes of the low-energy effective Hamiltonians, we have shown the significant reduction of the antiferromagnetic ordered moment occurs around $X = \text{EtMe}_3\text{Sb}$. This reduction is consistent with the experimentally observed quantum spin liquid behavior in $X = \text{EtMe}_3\text{Sb}$. We have also shown that the reduction is induced by both the geometrical frustration in the hopping integrals and off-site Coulomb interactions. This result indicates that accurate evaluation of the microscopic parameters in the Hamiltonians is essential for reproducing the quantum spin liquid behavior in the dmit-salts.

In addition to the *ab initio* study for the dmit-salts, we have also analyzed the long-range spin transport in the topological Dirac semimetals [9] using the real-time evolution of the quantum systems. Furthermore, using $\mathcal{H}\Phi$ [7, 8], we have analyzed the magnetization process of the antiferromagnetic Heisenberg model on the kagome lattice [10]. We have also developed an open-source library for the shifted Krylov subspace method ($K\omega$) [11] and an *Ab initio* tool for derivation of effective

low-energy model for solids (RESPACK) [5, 6].

References

- [1] R. Kato, Chem. Rev. **104**, 5319 (2004).
- [2] K. Kanoda, R. Kato, Annu. Rev. Condens. Matter Phys. **2**, 167 (2011).
- [3] T. Misawa, K. Yoshimi, T. Tsumuraya, Phys. Rev. Research **2**, 032072 (2020).
- [4] P. Giannozzi, O. Andreussi, T. Brumme, O. Bunau, M. B. Nardelli, M. Calandra, R. Car, C. Cavazzoni, D. Ceresoli, M. Cococcioni, et al., Journal of Physics: Condensed Matter **29**, 465901 (2017).
- [5] <https://sites.google.com/view/kazuma7k6r>
- [6] K. Nakamura, Y. Yoshimoto, Y. Nomura, T. Tadano, M. Kawamura, T. Kosugi, K. Yoshimi, T. Misawa, Y. Motoyama, Computer Physics Communications **261**, 107781 (2021).
- [7] M. Kawamura, K. Yoshimi, T. Misawa, Y. Yamaji, S. Todo, N. Kawashima, Comput. Phys. Commun. **217**, 180 (2017).
- [8] <https://www.pasums.issp.u-tokyo.ac.jp/HPhi/en/>
- [9] Y. Araki, T. Misawa, K. Nomura, arXiv:2103.06519.
- [10] T. Misawa, Y. Motoyama, Y. Yamaji, Phys. Rev. B **102**, 094419 (2020).
- [11] T. Hoshi, M. Kawamura, K. Yoshimi, Y. Motoyama, T. Misawa, Y. Yamaji, S. Todo, N. Kawashima, T. Sogabe, Computer Physics Communications **258**, 107536 (2021).

Study of phase formation, transport phenomena and effects of exceptional points in strongly correlated quantum systems

Norio KAWAKAMI

Department of Physics,

Kyoto University, Kitashirakawa, Sakyo-ku, Kyoto 606-8502

We have studied phase formation and transport phenomena in strongly correlated quantum systems. Especially, we have focused on phenomena such as the formation of magnetic phases and the effect of exceptional points when the non-Hermitian aspect of quasiparticle bands with finite lifetimes becomes essential.

(1) Open quantum systems

We have discussed the circumstances and requirements for the emergence of non-Hermitian phenomena in equilibrium single-particle properties of strongly correlated systems and their relationship to non-Hermitian phenomena in open quantum systems (OQS) experiencing gain and loss. While the necessity of postselection has limited the practicality of studying non-Hermitian phenomena in the OQS, in closed equilibrium systems, the single-particle Green's function is described by an effective non-Hermitian Hamiltonian without the need of postselection. By describing quasiparticles of strongly correlated systems as an OQS, we demonstrated that the non-Hermitian Hamiltonian arising in OQS and Green's functions are equivalent. We have also demonstrated the necessity of considering the memory effect in the quantum master equation by comparing the spectral function in the Hubbard model computed by an OQS and

equilibrium approaches.[1]

(2) Non-Hermitian phenomena

Quasiparticles described by Green's functions of equilibrium systems exhibit non-Hermitian topological phenomena because of their finite lifetime. This non-Hermitian perspective on equilibrium systems provides new insights into correlated systems. We provided a concise review of the non-Hermitian topological band structures for quantum many-body systems in equilibrium as well as their classification.[2]

Non-Hermitian phenomena offer a novel approach to analyze and interpret spectra in the presence of interactions. Using the density-matrix renormalization group (DMRG), we demonstrated the existence of exceptional points for the one-particle Green's function of the 1D alternating Hubbard chain with chiral symmetry, with a corresponding Fermi arc at zero frequency in the spectrum. They are robust and can be topologically characterized by the zeroth Chern number. This effect illustrates a case where the temperature has a strong impact in 1D beyond the simple broadening of spectral features. Furthermore, we demonstrated that exceptional points appear even in the two-particle Green's function (charge structure factor), where an effective Hamiltonian is difficult to establish.[3]

(3) Two-dimensional materials

The magnetic properties of black phosphorene nanoribbons have been investigated using static and dynamical mean-field theory. Besides confirming the existence of ferromagnetic/antiferromagnetic edge magnetism, our detailed calculations using large unit-cells find a phase transition at weak interaction strength to a novel incommensurate magnetic phase. Furthermore, we demonstrated that the difference of the ground state energies of the AFM and FM phase is exponentially small, making it possible to switch between both states by a small external field.[4]

We investigated the spin-dependent thermoelectric effect of graphene flakes with magnetic edges in the ballistic regime. Employing static and dynamical mean-field theory, we first showed that magnetism appears at the zigzag edges for a window of Coulomb interactions that increases significantly with increasing flake size. We then used the Landauer formalism in the framework of the non-equilibrium Green's function method to calculate the spin and charge currents in magnetic hexagonal graphene flakes by varying the temperature of the junction for different flake sizes. While in non-magnetic gated graphene, the temperature gradient drives a charge current, we observe a significant spin current for hexagonal graphene flakes with magnetic zigzag edges. Specifically, we showed that in the "meta" configuration of a hexagonal flake subject to weak Coulomb interactions, a pure spin current can be driven just by a temperature gradient in a temperature range that is promising

for device applications.[5]

(4) Many-body localization

Strong disorder in low-dimensional strongly correlated systems has been discussed to induce many-body localization, which is the localization of all many-body eigenstates of the Hamiltonian. However, it has been an open issue to precisely determine the critical strength of disorder at the localization phase transition in one or higher spatial dimensions. We have considered the Fock-space localization of many-body wavefunctions in an all-to-all interacting model of fermions and demonstrated a quantitative agreement of the numerically obtained moments of eigenstate wavefunctions as well as the spectral statistics to analytical predictions.[6]

References

- [1] Y. Michishita, and R. Peters, *Phys. Rev. Lett.* **124**, 196401 (2020).
- [2] T. Yoshida, R. Peters, N. Kawakami, and Y. Hatsugai, *Prog. Theor. Exp. Phys.* 12A109 (2020).
- [3] R. Rausch, R. Peters, and T. Yoshida, *New J. Phys.* **23**, 013001 (2021).
- [4] J. Vahedi and R. Peters, *Phys. Rev. B* **103**, 075108 (2021).
- [5] T. T. Phung, R. Peters, A. Honecker, G. T. de Laissardiere, and J. Vahedi, *Phys. Rev. B* **102**, 035160 (2020).
- [6] F. Monteiro, T. Micklitz, M. Tezuka, and A. Altland, *Phys. Rev. Research* **3**, 013023 (2021).

Theoretical study of correlated electron systems with strong spin-orbit coupling

Yukitoshi MOTOME

Department of Applied Physics,

The University of Tokyo, Bunkyo, Tokyo 113-8656

We have theoretically studied a variety of intriguing phenomena in correlated electron systems with spin-orbit coupling, ranging from Mott insulators to metals. During the last fiscal year, we have achieved substantial progress on the following topics (project numbers: 2020-Ca-0059 and 2020-Cb-0038). We summarize the main results below.

(i) Topological spin crystals: We clarified that interplay between spin, charge, and orbital degrees of freedom plays a crucial role in stabilizing the magnetic hedgehog crystals recently found in $B20$ chiral magnets [1]. We also showed that the spin-charge interplay gives rise to a square-lattice type skyrmion crystals [2]. Based on the results, we made a collaboration with the experimental group to clarify the importance of the spin-charge coupling in GdRu_2Si_2 hosting the square skyrmion crystal [3,4]. We also studied the effect of anisotropy in a triangular lattice system [5]. In addition, we investigated the effects of the spatial anisotropy [6], the phase shift [7], and the twist angle [8] on the topological spin crystals. We wrote a review paper on the itinerant frustration which is a

relevant mechanism to understand recent new generation of the topological spin crystals [9].

(ii) Kitaev quantum spin liquids: By using the quantum Monte Carlo simulation in the Majorana fermion representation, we investigated the effect of randomness on the Kitaev model for the thermodynamics and thermal transport [10] and the spin dynamics [11]. We also studied the finite-temperature phase transitions in a variety of three-dimensional extensions of the Kitaev model [12]. In addition, by using *ab initio* based calculations, we performed a systematic study of Pr-based f -electron compounds as new Kitaev candidates [13]. Summarizing our recent studies of the physics of Kitaev spin liquids and the material design of the Kitaev magnets, we wrote two review papers [14,15].

(iii) Spin-orbit physics not requiring the spin-orbit coupling: We showed that κ -type organic antiferromagnets exhibit an anomalous Hall response because of an effective spin-orbit coupling generated by glide symmetry breaking by the antiferromagnetic order [16]. We also showed that a similar mechanism predicts a spin current generation in perovskites with the

C-type antiferromagnetic order [17].

(iii) *Multipole physics*: We proposed channel-selective non-Fermi liquid behavior in the two-channel Kondo lattice model under a magnetic field [18]. We also clarified optical Hall responses in spin-orbit coupled metals with magnetic cluster multipole orders [19].

(iv) *Collaboration with experimental groups*: In addition to [3,4], we made combined studies between our theory based on the *ab initio* calculations and experiment on topological materials [20,21].

References

- [1] S. Okumura, S. Hayami, Y. Kato, and Y. Motome, Phys. Rev. B **101**, 144416 (2020).
- [2] S. Hayami and Y. Motome, Phys. Rev. B **103**, 024439 (2021).
- [3] Y. Yasui *et al.*, Nat. Commun. **11**, 5925 (2020).
- [4] 東京大学大学院工学系研究科 プレスリリース, "電荷密度波で電子構造の「ねじれ」をスイッチする トポロジカル状態の高速制御に向けた新しい指針を開拓".
- [5] S. Hayami and Y. Motome, Phys. Rev. B **103**, 054422 (2021).
- [6] K. Shimizu, S. Okumura, Y. Kato, and Y. Motome, Phys. Rev. B **103**, 054427 (2021).
- [7] S. Hayami, T. Okubo, and Y. Motome, preprint (arXiv:2005.03168).
- [8] K. Shimizu, S. Okumura, Y. Kato, and Y. Motome, preprint (arXiv:2009.14569).
- [9] S. Hayami and Y. Motome, preprint (arXiv:2103.10647).
- [10] J. Nasu and Y. Motome, Phys. Rev. B **102**, 054437 (2020).
- [11] J. Nasu and Y. Motome, preprint (arXiv:2103.10549).
- [12] T. Eschmann, P. A. Mishchenko, K. O'Brien, T. A. Bojesen, Y. Kato, M. Hermanns, Y. Motome, and S. Trebst, Phys. Rev. B **102**, 075125 (2020).
- [13] S.-H. Jang, R. Sano, Y. Kato, and Y. Motome, Phys. Rev. Materials **4**, 104420 (2020).
- [14] Y. Motome, R. Sano, S.-H. Jang, Y. Sugita, and Y. Kato, J. Phys: Condens. Matter **32**, 404001 (2020), [Special Issue on Quantum Spin Liquids].
- [15] 求 幸年, 那須 讓治, 固体物理 **55**, 297 (2020).
- [16] M. Naka, S. Hayami, H. Kusunose, Y. Yanagi, Y. Motome, and H. Seo, Phys. Rev. B **102**, 075112 (2020).
- [17] M. Naka, Y. Motome, and H. Seo, Phys. Rev. B **103**, 125114 (2021).
- [18] K. Inui and Y. Motome, Phys. Rev. B **102**, 155126 (2020).
- [19] T. Sato, Y. Umimoto, Y. Sugita, Y. Kato, and Y. Motome, Phys. Rev. B **103**, 054416 (2021).
- [20] N. Mitsuishi *et al.*, Nat. Commun. **11**, 2466 (2020) [selected as FOCUS].
- [21] M. Onga *et al.*, Nano Letters **20**, 4625 (2020).

Study on newly discovered nickelate superconductivity

Yusuke NOMURA

RIKEN Center for Emergent Matter Science, 2-1 Hirosawa, Wako, 351-0198

The recent discovery of superconductivity in the doped nickelate $\text{Nd}_{0.8}\text{Sr}_{0.2}\text{NiO}_2$ has attracted much attention because the nickelates may serve as a cuprate analog superconductor [1]. Indeed, the electronic structure of the nickelate is similar to that of the cuprates in the sense that the strongly correlated x^2-y^2 orbital is present. However, as a crucial difference from the cuprates, which shows Mott insulating behavior, $R\text{NiO}_2$ ($R=\text{Nd}, \text{Pr}$) is not a Mott insulator due to the carrier doping from the rare-earth layer (self-doping) [2].

In the present study, we investigate the following fundamental questions: (A) Is it possible to design nickelates whose electronic structure is more similar to that of the cuprates? (B) Can we expect large magnetic exchange coupling J in the cuprate-analog nickelates?

For (A), using a concept of “block layers”, we perform a systematic materials design of layered nickelates. Then, we find several dynamically stable cuprate-analog nickelates [3]. In such nickelates, the self-doping is absent, and hence the x^2-y^2 orbital becomes half-filled. Therefore, the correlation effect will induce Mott insulating behavior in such d^9 nickelates. Using the d^9 nickelates, we can perform a fair comparison between the nickelates (Mott-

Hubbard-type material) and cuprates (charge-transfer-type material).

(B) Then, it is of great interest to investigate the strength of magnetic exchange coupling J in the d^9 nickelates. Note that a large value of J of about 130 meV is a characteristic feature of the cuprates. We study the J value in theoretically-designed $\text{RbCa}_2\text{NiO}_3$ and $A_2\text{NiO}_2\text{Br}_2$ (A : a cation with the valence of +2.5) (Fig. 1). We show that these nickelates have a sizeable magnetic exchange coupling as large as about 80-100 meV, which is not far smaller than that of the cuprates [4].

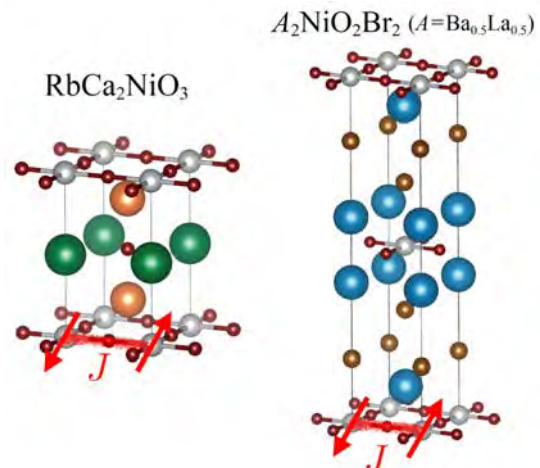


Fig. 1: Crystal structure of $\text{RbCa}_2\text{NiO}_3$ and $A_2\text{NiO}_2\text{Br}_2$ (A : a cation with the valence of +2.5).

References

- [1] D. Li *et al.*, Nature **572**, 624 (2019)
- [2] Y. Nomura *et al.*, Phys. Rev. B **100**, 205138 (2019) [Editor's suggestion]
- [3] M. Hirayama and T. Tadano *et al.*, Phys. Rev. B **101**, 075107 (2020)
- [4] Y. Nomura *et al.*, Phys. Rev. Research **2**, 043144 (2020).

Studies on superconductivity in multiorbital systems with an incipient band and designing of new nickelate superconductors

KAZUHIKO KUROKI

Department of Physics, Osaka University

1-1 Machikaneyama, Toyonaka, Osaka, 560-0043, Japan

SUPERCONDUCTING MECHANISM OF A NEW CUPRATE SUPERCONDUCTOR $\text{Ba}_2\text{CuO}_{3+\delta}$

Recently, Li et al.[1] reported high- T_c superconductivity in a new cuprate $\text{Ba}_2\text{CuO}_{3+\delta}$ with a K_2NiF_4 -like layered structure. There, they find several unique features which strongly suggest that the material is a different type of cuprate superconductor that opens up a new paradigm. Namely, a large amount of oxygen vacancies are present within the CuO_2 planes, and a great amount of holes are doped which should cause a large deviation of the Cu valence from 2+. Also, the distance between Cu and the apical O is shorter than the in-plane Cu-O distance, so that the octahedron is compressed along the c axis. This should result in a crystal field very different from that of the ordinary cuprates, namely, the $3d_{3z^2-r^2}$ orbital lifted in energy above the $3d_{x^2-y^2}$ orbital. These findings suggest that the mechanism of superconductivity in the $\text{Ba}_2\text{CuO}_{3+\delta}$ may be considerably different from that for the conventional cuprates.

In 2020 fiscal year, we have studied possible superconducting mechanisms of $\text{Ba}_2\text{CuO}_{3+\delta}$ [2]. In order to study the superconducting mechanism of the new superconductor, a realistic model Hamiltonian is required, which has to start with a determination of the crystal structure. For the 2-1-3 composition in particular, the chain structure is known to be stable in an actual material Sr_2CuO_3 . As another possibility within the 2-1-3 composition, we considered a Lieb lattice type structure. First principles total-energy calculation performed with the VASP code shows that the chain and the Lieb lattice structures are close in the total energy, so that the latter may also be considered as a candidate.

Focusing on these two structures, we have calculated their band structures, and extracted the Wannier orbitals to construct multiorbital Hubbard models, i.e, a two-orbital model for the chain structure and a six-orbital model for the Lieb type structure. We have applied fluctuation exchange approximation to the effective models, and discuss the possibility of superconductivity by solving the linearized Eliashberg equation. We have shown that s -wave and d -wave pairings closely compete with each other and, more interestingly, that a co-existence of intra- and interorbital pairings arises.

We also reveal an intriguing relation of the Lieb model with the two-orbital model for the usual K_2NiF_4 -type cuprate where a close competition between s - and d -wave pairings is known to occur.

We have further shown that $s\pm$ -wave superconductivity is strongly enhanced when the $d_{3z^2-r^2}$ band is raised in energy so that it become nearly incipient with the lower edge of the band close to the Fermi level within a realistic band filling regime. The enhanced superconductivity in the present model is in fact shown to be related to an enhancement found previously in the bilayer Hubbard model with an incipient band. Namely, we can show that, by orbital basis transformation[3], the two-orbital model can be transformed to the bilayer Hubbard model when all the intra and inter-orbital interactions have the same magnitude. In reality, the interactions are different in magnitude, but we find that the similarity between the two models holds to some extent. The strong enhancement of $s\pm$ -wave superconductivity in the bilayer model with an incipient band has been shown by a number of previous studies, including our numerical study[4] based on multi-variable variational Monte Carlo method[5, 6].

DESIGNING NICKELATE SUPERCONDUCTORS

Inspired by the proposed superconducting mechanism for $\text{Ba}_2\text{CuO}_{3+\delta}$, in 2020 fiscal year, we have also theoretically designed unconventional nickelate superconductors with d^8 electron configuration[7]. Although the materials that we design apparently have nothing to do with bilayer systems at first glance, electronic structure of these materials resemble that of the bilayer Hubbard model, thereby strongly enhancing superconductivity. It is known that bilayer Hubbard model with appropriately large interlayer electron hopping exhibits $s\pm$ -wave superconductivity with extremely high- T_c , but it is generally difficult to realize such a situation in actual bilayer-type materials due to various restrictions regarding the atomic orbitals. We have adopted a completely different strategy to realize the desired situation, by which we design a mixed-anion nickelates as candidates for new high- T_c superconductors.

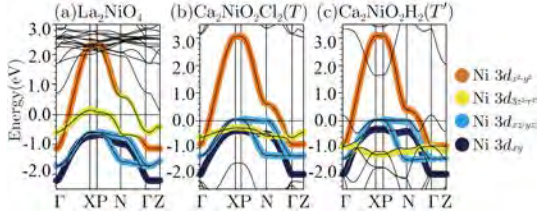


FIG. 1. Band structures of (a) La_2NiO_4 , (b) $\text{Ca}_2\text{NiO}_2\text{Cl}_2$ and (c) $\text{Ca}_2\text{NiO}_2\text{H}_2$ (taken from Ref.[7]).

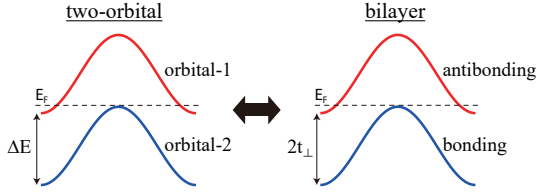


FIG. 2. Schematic figure of the correspondence between the two-orbital model and the bilayer model (taken from Ref.[7]).

More specifically, we have considered d^8 nikelates with K_2NiF_4 structure, where the apical oxygens are replaced by halogens or hydrogens. The lattice parameters are determined by structural optimization using VASP. The band structures of two of the proposed candidates, $\text{Ca}_2\text{NiO}_2\text{Cl}_2$ and $\text{Ca}_2\text{NiO}_2\text{H}_2$, are shown in Fig.1 together with that of a reference material La_2NiO_4 . The key point here is that the large crystal field splitting of the orbital energy levels, induced by replacing the apical oxygens by halogens or hydrogens, is approxi-

mately equivalent to large interlayer hopping in a bilayer system, as schematically depicted in Fig.2. Applying the fluctuation exchange approximation to the five orbital model of these materials, we have shown that the maximum superconducting transition temperature of some of them may be even higher than that of the high- T_c cuprates.

We have further found that our theory may also be related to another newly discovered superconductor $(\text{Nd,Sr})\text{NiO}_2$ [8]. In this superconductor, the nickel electron configuration is expected to be close to d^9 , but this might be affected, e.g., by the reduction process during the synthesis of the material. Since the band structure of $(\text{Nd,Sr})\text{NiO}_2$ itself, due to the absence of apical oxygens, resembles that of the proposed mixed anion-nikelates, (unintentional) reduction of the electron number in $(\text{Nd,Sr})\text{NiO}_2$ may also result in a similar $s\pm$ -wave superconductivity.

-
- [1] W.M. Li *et al.*, Proc. Natl. Acad. Sci. USA **116**, 12156 (2019).
 - [2] K. Yamazaki *et al.* Phys. Rev. Res. **2**, 033356 (2020).
 - [3] H. Shinaoka *et al.*, Phys. Rev. B **92**, 195126 (2015).
 - [4] D. Kato and K. Kuroki, Phys. Rev. Res. **2**, 023156 (2020).
 - [5] D. Tahara and M. Imada, J. Phys. Soc. Jpn. **77**, 114701 (2008).
 - [6] T. Misawa *et al.*, Comp. Phys. Comm. **235**, 447 (2019).
 - [7] N. Kitamine, M. Ochi and K. Kuroki, Phys. Rev. Res. **2**, 042032(R).
 - [8] D. Li *et al.*, Nature (London) **572**, 624 (2019).

Bulk-edge correspondence for non-Hermitian topological systems

Tsuneya Yoshida

Department of Physics,

1-1-1 Tennodai, Tsukuba, Ibaraki, JAPAN 305-8571

In this year, we have studied topological phases in non-Hermitian systems [1-6]. In particular, by employing numerical diagonalization of a non-Hermitian matrix, we have elucidated the topological properties of non-Hermitian fractional quantum Hall state [1].

Specifically, we have analyzed a two-dimensional open quantum system with two-body loss. Such a system is described by Lindblad equation. Vectorizing the density matrix, we have mapped the Liouvillian to the Liouvillian matrix. Diagonalizing this matrix, we have analyzed topological properties. Our analysis elucidate that for a system with two-body loss, the Liouvillian gap remains open (see Fig. 1). In addition, introducing the pseudo-spin Chern number, we have elucidated that topology of non-Hermitian fractional quantum Hall states is maintained for this open quantum systems.

Our approach of the characterization can be also generalized to other cases of

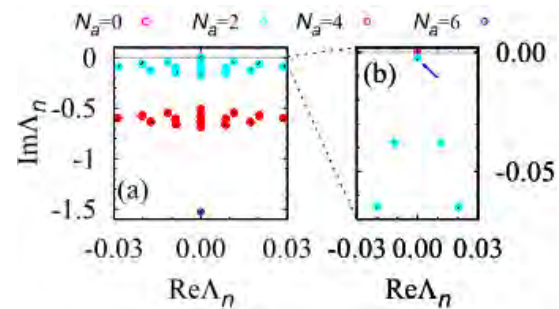


Fig.1 Spectrum of the Liouvillian matrix describing fractional non-Hermitian quantum Hall states.

dimensions and symmetry, e.g., one dimensional open quantum systems with inversion symmetry.

We have also analyzed classical systems in term of topological band theory[7-9]. Our analysis have elucidated that topological phenomena are observed a variety of systems beyond quantum systems.

References

- [1] T. Yoshida, K. Kudo, H. Katsura, and Y. Hatsugai, *Phys. Rev. Research* **2** 033428 (2020)
- [2] T. Yoshida, *Phys. Rev. B* **103** 125145 (2021).

- [3] H. Araki, T. Yoshida, and Y. Hatsugai, (2020).
J. Phys. Soc. Jpn. **90** 053703 (2021).
- [4] P. Delplace, T. Yoshida, Y. Hatsugai,
arXiv: 2103.08232.
- [5] R. Rausch, R. Peters, and T. Yoshida,
New J. Phys. **23** 013011 (2021).
- [6] T. Yoshida, T. Mizoguchi, and Y.
Hatsugai Phys. Rev. Research **2** 022062 .
- [7] T. Yoshida, T. Mizoguchi, and Y.
Hatsugai arXiv:2012.05562.
- [8] T. Yoshida, T. Mizoguchi, Y. Kuno and
Y. Hatsugai arXiv: 2103.11305
- [9] T. Yoshida and Y. Hatsugai, Sci. Rep.
11 888 (2021).

Numerical analyses on quantum spin liquids in strongly correlated electron systems

Kota IDO

Institute for Solid State Physics,

The University of Tokyo, Kashiwa-no-ha, Kashiwa, Chiba 277-8581

β' -Pd(dmit)₂ salts have attracted attention as candidate materials where a quantum spin liquid emerges [1]. This system consists of the dimers of two Pd(dmit)₂ molecules and cations. Since the dimers form an anisotropic triangular lattice, this system is considered as a two-dimensional correlated electron system with strong geometrical frustration. Although numerical studies play an important role in interpreting experimental results in the candidate materials for quantum spin liquids, it is difficult to accurately analyze large two-dimensional systems with strong frustration and many-body correlations.

In this study, to perform the ground state analysis on strongly correlated electron systems with geometrical frustration, we improved the accuracy of the trial wavefunction of the variational Monte Carlo (VMC) method. To achieve this goal, we proposed a two-component pairing wavefunction as the fermionic wavefunction. The difference from the conventional pairing wavefunction is that the strength of the pairing is dependent on the number of the local density. By using this wavefunction combined with recently developed neural network correlators [2, 3], we performed benchmarks for the t - t' Hubbard model on the square lattice and the triangular lattice with one-dimensional anisotropy. We

find that the energy of quantum spin liquids using our proposed wavefunction is much lower than those using the conventional pairing wavefunction. In addition, we performed variance extrapolations of energies by using the power Lanczos method [4]. As the results, we succeed in reproducing the stability of the quantum spin liquid obtained by using the fixed-node method [5]. Our results suggest that this approach is a new efficient way to analyze the ground state in strongly correlated electron systems with the geometrical frustration and to clarify the nature of the spin liquids.

In addition, we have analyzed the ground states of an extended Kitaev model using the VMC method. It is a future issue to study not only the ground states but also nonequilibrium phenomena in quantum spin liquids.

References

- [1] K. Kanoda, R. Kato, *Annu. Rev. Condens. Matter Phys.* **2**, 167 (2011).
- [2] G. Carleo and M. Troyer, *Science* **355**, 602 (2017).
- [3] Y. Nomura, A. S. Darmawan, Y. Yamaji, and M. Imada, *Phys. Rev. B* **96**, 205152 (2017).
- [4] E. S. Heeb, T. M. Rice, *Z. Phys. B* **90**, 73 (1993).
- [5] L. F. Tocchio, A. Parola, C. Gros, and F. Becca, *Phys. Rev. B* **80**, 064419 (2009).

Search for multiple- Q magnetic orders in systems with bond-dependent anisotropic interactions

Satoru Hayami

Department of Applied Physics, The University of Tokyo, Tokyo 113-8656

Noncoplanar spin textures have attracted considerable attention for potential applications to next-generation electronic and spintronic devices. In the project with numbers: 2020-Ca-0002 and 2020-Cb-0005, we have theoretically investigated a plethora of noncoplanar spin textures in correlated electron systems. We have presented the main results this year below.

(i) Magnetic hedgehog lattice: A magnetic hedgehog lattice (HL), which is characterized by a periodic array of magnetic monopoles and antimonopoles, is one of the noncoplanar multiple- Q states in the three-dimensional lattice system. The emergence of the HLs has been suggested in the noncentrosymmetric metal $\text{MnSi}_{1-x}\text{Ge}_x$ [1, 2] by experiments, but their microscopic origins have not been fully clarified owing to the unconventional short magnetic periods of the spin textures. We have investigated the stability of the HLs by analyzing an effective spin model derived from an itinerant electron model [3]. By using the variational calculations and simulated annealing, we obtained two types of HLs in the wide range of model parameters in the ground-state phase diagram. The results indicate the importance of the interplay between the Dzyaloshinskii-Moriya(DM)-type interaction by the spin-orbit coupling and the multiple-spin interactions by the spin-charge coupling.

(ii) Square skyrmion crystal: We have studied an instability toward a square skyrmion crystal (SkX), which consists of two helices with equal weight, in a centrosym-

metric tetragonal lattice system [4]. We considered an effective spin model from an itinerant electron model on a square lattice. Reflecting the itinerant nature of electrons, the spin model exhibits the bilinear and biquadratic interactions in momentum space [5]. We also introduced fourfold-symmetric bond-dependent anisotropic and easy-axis anisotropic interactions to stabilize the multiple- Q states. By performing simulated annealing, we have shown that the square SkX appears by the synergy effect among the biquadratic, bond-dependent anisotropic, and easy-axis anisotropic interactions in an external magnetic field. We have also shown that the magnetic phase diagram obtained by simulated annealing well reproduces the experimental results for the SkX hosting material GdRu_2Si_2 [6, 7].

In addition, we have investigated the vorticity and helicity of the square SkX in centrosymmetric itinerant magnets. Owing to the absence of the DM interaction in centrosymmetric magnets, the vorticity and helicity of the SkX are arbitrary. In other words, the Néel SkX, Bloch SkX, and two anti-SkXs are degenerate. In such a situation, we found that the anisotropic Ruderman-Kittel-Kasuya-Yosida (RKKY) interaction depending on the wave vectors lift the degeneracy of the SkXs with the different vorticity and helicity [8]. Our result opens a possibility of controlling the types of the SkXs through the electronic band structures.

(iii) Triangular skyrmion and meron crys-

tals: We have studied the SkXs and meron crystals in itinerant hexagonal magnets [9]. On the basis of the effective spin model with the bilinear and biquadratic interactions in momentum space [5], we examined the effect of two magnetic anisotropies on the stability of the multiple- Q states: The one is the local single-ion anisotropy and the other is the sixfold-symmetric bond-dependent anisotropy. In the case the single-ion anisotropy, we found that both the SkXs with the skyrmion number of one and two, which are denoted as the $n_{\text{sk}} = 1$ SkX and $n_{\text{sk}} = 2$ SkX, appear under the single-ion anisotropy, although their stability against the single-ion anisotropy is different with each other. For the $n_{\text{sk}} = 2$ SkX, it is found that the stable region under the easy-axis anisotropy is wider than that for the easy-plane anisotropy at zero field. Meanwhile, the critical magnetic field to destabilize the $n_{\text{sk}} = 2$ SkX is larger for the easy-plane anisotropy than that for the easy-axis anisotropy. For the $n_{\text{sk}} = 1$ SkX, there is a drastic effect of the single-ion anisotropy on its stability; the $n_{\text{sk}} = 1$ SkX is very weak (strong) against the easy-plane(-axis) anisotropy.

Under the bond-dependent anisotropy, we also obtained both the $n_{\text{sk}} = 1$ and $n_{\text{sk}} = 2$ SkXs in the wide range of model parameters. Notably, we found a variety of chiral magnetic states with nonzero scalar chirality, which is distinct from the SkXs. Especially, we obtained two types of the meron crystals: One is the $n_{\text{sk}} = 1$ meron crystal, which consists of one meron-like and three antimerion-like spin textures in the magnetic unit cell and the other is the $n_{\text{sk}} = 2$ meron crystal consisting of four meron-like spin textures in the magnetic unit cell.

The effective spin model in itinerant magnets will provide a deep understanding of the mechanism of the multiple- Q states, which have been recently observed in experiments, in an efficient way. Indeed, we reproduced the magnetic phase diagrams in $\text{Gd}_3\text{Ru}_4\text{Al}_{12}$ [10]

and CeAuSb_2 [11], which host the multiple- Q states, by analyzing the extended effective spin model.

References

- [1] T. Tanigaki *et al.*, Nano Lett. **15** (2015) 5438.
- [2] Y. Fujishiro *et al.*, Nat. Commun. **10** (2019) 1059.
- [3] S. Okumura, S. Hayami, Y. Kato, and Y. Motome, Phys. Rev. B **101** (2020) 144416.
- [4] S. Hayami and Y. Motome, Phys. Rev. B **103** (2021) 024439.
- [5] S. Hayami, R. Ozawa, and Y. Motome, Phys. Rev. B **95** (2017) 224424.
- [6] N. D. Khanh *et al.*, Nat. Nanotech. **15** (2020) 444.
- [7] Y. Yasui *et al.*, Nat. Commun. **11** (2020) 5925.
- [8] S. Hayami and R. Yambe, J. Phys. Soc. Jpn. **89** (2020) 103702.
- [9] S. Hayami and Y. Motome, Phys. Rev. B **103** (2021) 054422.
- [10] M. Hirschberger, S. Hayami, and Y. Tokura, New J. Phys. **23** (2021) 023039.
- [11] S. Seo *et al.*, Commun. Phys. **4** (2021) 58.

Time-Dependent DMRG Study of Spectral Shape in the Optical Conductivity of Two-Dimensional Hubbard Model

Takami TOHYAMA

Department of Applied Physics, Tokyo University of Science, Tokyo 125-8585

The parent compound of cuprate superconductors is a Mott insulator in two dimensions. The optical conductivity in the compound has been measured and its spectral features have been discussed experimentally. However, theoretical understanding of its spectral shape is still far from complete. This is due to theoretical difficulty caused by strong coupling of localized spins and holon/doublon created by photoexcitations. For example, it is unclear whether there is a magnetically induced excitonic peak at the absorption edge or not [1, 2].

In order to clarify spectral properties of the optical conductivity in two-dimensional Mott insulator, we use time-dependent density-matrix renormalization group (tDMRG) technique for a half-filled Hubbard model with second-neighbor hopping (t - t' - U model) and calculate time-dependent current induced by electric field applied along the x direction, from which we can obtain the optical conductivity. In our tDMRG the time-evolution operator necessary for the calculation of time-dependent wave function is evaluated by using a kernel polynomial method [3], which is an approach good for lattices more than one dimension.

We use a 6×6 square lattice of the t - t' - U model with $U/t = 10$ under open boundary condition [4]. The number of states kept in tDMRG procedure is 4000. We note that we also use an 8×8 lattice to check size dependence for a t - U model and find that the difference of the optical conductivity in the two lattices is small. For the 6×6 lattice without

t' , the optical conductivity shows a prominent peak at the absorption edge followed by continuous spectral weight distribution above the peak position. The peak intensity depends on the value of t' , exhibiting a maximum of the peak intensity at $t' = 0$ as a function of t' . Since t' introduces a diagonal antiferromagnetic exchange interaction, the effect of frustration competing with the nearest-neighbor exchange interaction appears. The frustration effect should not be dependent on the sign of t' . This is the case of the present result. We can say that magnetic interactions contribute to the peak at the absorption edge, indicating magnetic origin of the peak, i.e., magnetic exciton. However, we note that there is no gap between the peak and continuum mentioned above. This is different from a standard exciton where the exciton is defined as a bound state with well-defined binding energy.

References

- [1] T. Tohyama, Y. Inoue, K. Tsutsui, and S. Maekawa: Phys. Rev. B **72** (2005) 045113.
- [2] X.-J. Hana *et al.*: New J. Phys. **18** (2016) 103004.
- [3] K. Shinjyo and T. Tohyama: Phys. Rev. B **103** (2021) 035141.
- [4] K. Shinjyo, Y. Tamaki, S. Sota, and T. Tohyama, in preparation.

Development and application of DFT+DMFT software DCore

Hiroshi SHINAOKA

*Department of Physics, Saitama University,
Saitama 338-8570*

Dynamical mean-field theory (DMFT) has become a standard theoretical tool for studying strongly correlated electronic systems. In a DMFT calculation, an original lattice model is mapped to an effective Anderson impurity problem whose bath degrees of freedom are self-consistently determined. Although the DMFT was originally proposed for solving models such as Hubbard models, it can be combined with density functional theory (DFT) based on *ab initio* calculations for describing the electronic properties of strongly correlated materials. This composite framework, called DFT+DMFT, has been applied to various types of materials.

To make DFT+DMFT available to more users and to promote the development of a community of users and developers, we need an open-source program package with a user-friendly interface.

In this project, we have developed an open-source program, DCore v3.0.0 [1], that implements DMFT. This program features an interface based on text and HDF5 files, allowing DMFT calculations of tight-binding models to be performed on predefined lattices as well as first-principles models constructed by external DFT codes through the Wannier90 package. Furthermore, DCore provides interfaces to a variety of quantum impurity solvers such as quantum Monte Carlo codes developed in the ALPS projects. DCore is implemented on the top of the TRIQS Python library (Toolbox for Research on Interacting Quantum Systems). DCore v3.0.0 supports Python 3.x and TRIQS 3.0.

We used DCore to generate hybridization functions for a five-orbital 2×2 cluster impurity model for LaAsFeO [2]. The impurity model involves 40 spin orbitals. The hybridization functions computed by DCore are shown in Fig. 1. The hybridization functions have large off-diagonal elements and decay exponentially in the intermediate representation (IR) basis. We found that the exact hybridization functions with large off-diagonal elements can be fitted accurately with 332 bath sites using sparse modeling techniques.

This report is based on the collaboration with Y. Nagai, J. Otsuki, M. Kawamura, N. Takemori, K. Yoshimi.

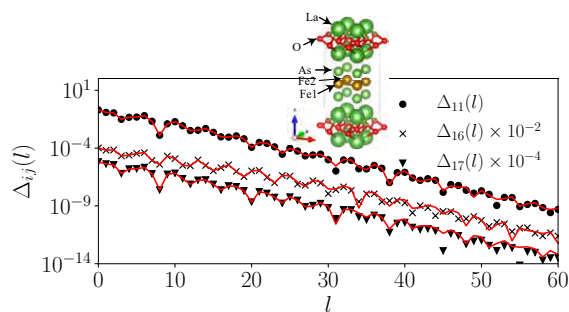


Figure 1: Illustration of the DMFT self-consistency cycle implemented in DCore

References

- [1] H. Shinaoka, J. Otsuki, M. Kawamura, N. Takemori, K. Yoshimi, arXiv:2007.00901v3
- [2] H. Shinaoka and Y. Nagai, PRB **103**, 045120 (2021)

Classical Monte Carlo study of J_1 - J_2 Heisenberg antiferromagnet on the kagome lattice

Hiroshi SHINAOKA

*Department of Physics, Saitama University,
Saitama 338-8570*

Frustrated XY antiferromagnets have been investigated extensively in the past decades due to exotic phenomena induced by geometrical frustration. The classical nearest-neighbor XY antiferromagnet on the kagome lattice is a typical two-dimensional frustrated magnet. This model hosts a macroscopically degenerate ground-state manifold. Small perturbations such as thermal fluctuations lift the macroscopic degeneracy. This gives rise to various exotic phenomena. An interesting question is how next-nearest-neighbor interaction affects the competition of degenerated states at finite temperature.

In this project, we investigated the finite-temperature phase diagram of classical J_1 - J_2 XY antiferromagnets on the kagome lattice through extensive Monte Carlo simulations [1, 2] using loop updates. We implemented the code in Julia, which is a modern programming language for scientific computing. The code is parallelized using MPI.jl.

We found that a weak antiferromagnetic J_2 induces an unconventional first-order transition at low temperatures. Furthermore, in the vicinity of the first-order transition, we find an octupole ordered phase between two competing quasi-long-range orders with different spin configurations (See Fig. 1). At antiferromagnetic $J_2 = -0.03$, the ground state is the $q = 0$ state. As shown in Fig. 2, there is a first-order transition between the high-temperature paramagnetic phase and the $q = 0$ quasi-long-range-ordered phase. At $J_2 = -0.005$, the Berezinskii-Kosterlitz-Thouless transition appears at a higher temperature. This report is

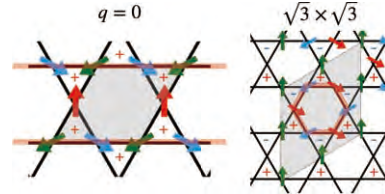


Figure 1: $q = 0$ and $\sqrt{3} \times \sqrt{3}$ spin configurations

based on the collaboration with F. Kakizawa and T. Misawa.

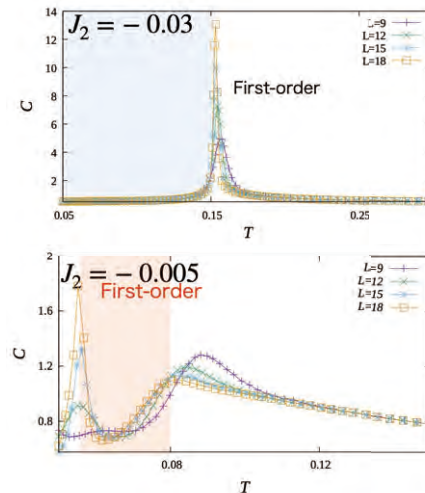


Figure 2: Temperature (T) dependence of the specific heat C computed for $J_2 = -0.03$ and $J_2 = -0.005$

References

- [1] F. Kakizawa, T. Misawa, H. Shinaoka, APS March Meeting 2021, Y39.00012.
- [2] 柿澤文哉, 三澤貴宏, 品岡寛, J_1 - J_2 古典反強磁性 XY カゴメ模型における新奇相転移、日本物理学会第76回年次大会(2021年), 12pC1-8.

Research of Quantum Critical Points Emerging between Two-Channel Kondo and Fermi-Liquid States

Takashi HOTTA

*Department of Physics, Tokyo Metropolitan University
1-1 Minami-Osawa, Hachioji, Tokyo 192-0397*

In this research, we have investigated the emergence of quantum critical points (QCP) near a two-channel Kondo phase by evaluating an f -electron entropy of a seven-orbital impurity Anderson model hybridized with three (Γ_7 and Γ_8) conduction bands with the use of a numerical renormalization group (NRG) method.

First we consider the local f -electron Hamiltonian H_{loc} . For the purpose, we introduce one f -electron state, which is defined by the eigenstate of spin-orbit and crystalline electric field (CEF) potential terms. Under the cubic CEF potential, we obtain Γ_7 doublet and Γ_8 quartet from $j = 5/2$ sextet, whereas we find Γ_6 doublet, Γ_7 doublet, and Γ_8 quartet from $j = 7/2$ octet. By using those one-electron states as bases, we describe H_{loc} as

$$\begin{aligned}
 H_{\text{loc}} = & \sum_{j,\mu,\tau} (\lambda_j + B_{j,\mu} + E_f) f_{j\mu\tau}^\dagger f_{j\mu\tau} \\
 & + \sum_{j_1 \sim j_4} \sum_{\mu_1 \sim \mu_4} \sum_{\tau_1 \sim \tau_4} I_{\mu_1 \tau_1 \mu_2 \tau_2, \mu_3 \tau_3 \mu_4 \tau_4}^{j_1 j_2, j_3 j_4} \quad (1) \\
 & \times f_{j_1 \mu_1 \tau_1}^\dagger f_{j_2 \mu_2 \tau_2}^\dagger f_{j_3 \mu_3 \tau_3} f_{j_4 \mu_4 \tau_4},
 \end{aligned}$$

where $f_{j\mu\tau}$ denotes the annihilation operator of a localized f electron in the bases of (j, μ, τ) , j is the total angular momentum, $j = 5/2$ and $7/2$ are denoted by “ a ” and “ b ”, respectively, μ distinguishes the cubic irreducible representation, Γ_8 states are distinguished by $\mu = \alpha$ and β , while Γ_7 and Γ_6 states are labeled by $\mu = \gamma$ and δ , respectively, τ is the pseudo-spin which distinguishes the degeneracy concerning the time-reversal symmetry, and E_f is the f -

electron level to control the local f -electron number at an impurity site.

As for the spin-orbit coupling term, we obtain $\lambda_a = -2\lambda$ and $\lambda_b = (3/2)\lambda$, where λ is the spin-orbit coupling of f electron. In this research, we set $\lambda = 0.1$ and 0.11 for Pr and Nd ions, respectively. Concerning the CEF potential term for $j = 5/2$, we obtain $B_{a,\alpha} = B_{a,\beta} = 1320B_4^0/7$ and $B_{a,\gamma} = -2640B_4^0/7$, where B_4^0 denotes the fourth-order CEF parameter for the angular momentum $\ell = 3$. Note that the sixth-order CEF potential term B_6^0 does not appear for $j = 5/2$, since the maximum size of the change of the total angular momentum is less than six. On the other hand, for $j = 7/2$, we obtain $B_{b,\alpha} = B_{b,\beta} = 360B_4^0/7 + 2880B_6^0$, $B_{b,\gamma} = -3240B_4^0/7 - 2160B_6^0$, and $B_{b,\delta} = 360B_4^0 - 3600B_6^0/7$. Note also that B_6^0 term appears in this case. In the present calculations, we treat B_4^0 and B_6^0 as parameters.

Now we consider the matrix element I of the Coulomb interaction. Here we skip the details of the derivation of I , but they are expressed with the use of four Slater-Condon parameters, F^0 , F^2 , F^4 , and F^6 . Although the Slater-Condon parameters of a material should be determined from experimental results, here we simply set the ratio as $F^0/10 = F^2/5 = F^4/3 = F^6 = U$, where U is the Hund’s rule interaction among f orbitals. It is reasonable to set U as 1 eV in this research.

In Fig. 1, we show the local CEF ground-state phase diagram for $n = 3$, obtained from

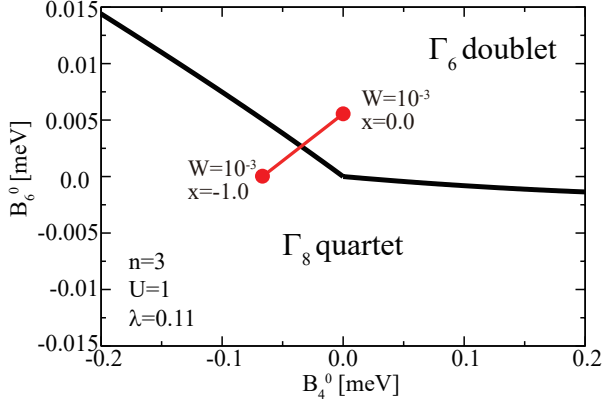


Figure 1: Local CEF ground-state phase diagram on the plane of (B_4^0, B_6^0) for $n = 3$. Red line denote the trajectory of $B_4^0 = Wx/15$ and $B_6^0 = W(1 - |x|)/180$ in the range of $-1 \leq x \leq 0$ for $W = 10^{-3}$.

the diagonalization of H_{loc} . For $n = 3$, the ground-state multiplet for $B_4^0 = B_6^0 = 0$ is characterized by total angular momentum $J = 9/2$. Under the cubic CEF potentials, the dectet of $J = 9/2$ is split into three groups as one Γ_6 doublet and two Γ_8 quartets.

Now we include the Γ_7 and Γ_8 conduction electron bands. Here we consider only the hybridization between conduction and $j = 5/2$ electrons. The Hamiltonian is given by

$$H = \sum_{\mathbf{k}, \mu, \tau} \varepsilon_{\mathbf{k}} c_{\mathbf{k}\mu\tau}^\dagger c_{\mathbf{k}\mu\tau} + \sum_{\mathbf{k}, \mu, \tau} V_\mu (c_{\mathbf{k}\mu\tau}^\dagger f_{a\gamma\tau} + \text{h.c.}) + H_{loc}, \quad (2)$$

where $\varepsilon_{\mathbf{k}}$ is the dispersion of conduction electron with wave vector \mathbf{k} , $c_{\mathbf{k}\gamma\tau}$ is an annihilation operator of conduction electrons, and V_μ denotes the hybridization between f electron in the μ orbital and conduction electron of the μ band. Here we set $V_\alpha = V_\beta = V_\gamma = V$.

In this research, we analyze this model by employing the NRG method [1]. We introduce a cut-off Λ for the logarithmic discretization of the conduction band. Due to the limitation of computer resources, we keep M low-energy states. Here we use $\Lambda = 8$ and $M = 5,000$. Note that the temperature T is defined as $T = D\Lambda^{-(N-1)/2}$ in the NRG calculation, where N

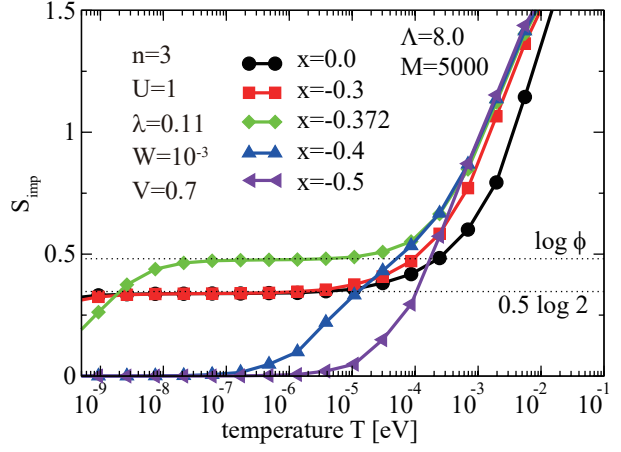


Figure 2: Entropies S_{imp} vs. temperature for $n = 3$ in the range of $-1 \leq x \leq 0$ with $W = 10^{-3}$. Note that ϕ is given by $\phi = (\sqrt{5} + 1)/2$.

is the number of the renormalization step and D is a half of conduction band width. Here we set $D = 1$ eV.

Here we briefly discuss the typical results for $n = 3$ [2]. In Fig. 2, we show entropies S_{imp} vs. temperature, when we change the CEF parameters from $x = 0$ (Γ_6 doublet) to $x = -1$ (Γ_8 quartet) for $n = 3$, $W = 0.001$, and $V = 0.7$. For $x = 0$ and -0.3 , we obtain the magnetic two-channel Kondo phase, while for $x = -0.4$ and -0.5 , the screened Kondo phase appears, since the Γ_8 quartet effectively expressed by $S = 3/2$ spin is screened by three conduction electrons. At $x = -0.372$ between two-channel Kondo and Fermi-liquid phases, we find an entropy plateau of $\log \phi$. In this case, we could not observe the residual entropy of $\log \phi$ at low enough temperatures, but the signal of QCP is considered to be obtained.

References

- [1] H. R. Krishna-murthy, J. W. Wilkins, and K. G. Wilson, Phys. Rev. B **21**, 1003 (1980).
- [2] T. Hotta, J. Phys. Soc. Jpn. **89**, 114706 (2020).

Disorder effect on Kitaev quantum spin liquids

Joji Nasu

*Department of Physics, Yokohama National University
Hodogaya, Yokohama 240-8501, Japan*

Quantum spin liquid has been actively studied in strongly correlated electron systems. It is a state that does not show magnetic order down to the lowest temperature, which appears in insulating magnets and thought to appear owing to the cooperation of strong quantum fluctuations and many-body effects. Thus far, one considers geometrical frustration, which is essential to realize this state in the Heisenberg quantum spin model in the lattice structure. However, in this situation, one usually suffers from the negative sign problem in the quantum Monte Carlo method. Hence, the properties of quantum spin liquid have not been well understood theoretically.

On the other hand, attempts to realize quantum spin liquids other than the Heisenberg model have been made. Among them, the Kitaev model has recently attracted considerable attention because its ground state is a quantum spin liquid as an exact solution. Experimentally, many physical quantities such as specific heat, entropy, magnetic excitation, and thermal transport properties have been measured in ruthenium and iridium compounds, which are believed to be described by the Kitaev model, and have been compared with theoretical studies. In the real systems, effects of the disorder are inevitably present, which complicates extracting the nature of the Kitaev quantum spin liquid. Thus, calculations incorporating such effects are necessary to separate the properties intrinsic to Kitaev quantum spin liquids from others.

In this study, we perform numerical calculations for the Kitaev model with site dilution

and bond randomness using quantum Monte Carlo simulations. The spin Hamiltonian is rewritten into the free Majorana fermion system coupled to Z_2 variables. The Majorana fermion system is diagonalized using the LAPACK library, and the configurations of the Z_2 variables are updated by the Markov chain Monte Carlo method. To avoid the freezing of the configurations, we employ the parallel tempering technique using the MPI library. Here, we calculate thermodynamic quantities such as the specific heat and thermal transport [1]. We find that the specific heat remains largely intact even in the presence of disorder at higher temperatures compared to the spin-exchange energy, while the low-temperature behavior is sensitive to the disorder. For thermal transport, the longitudinal component of the thermal conductivity is suppressed by the disorder. This behavior is common to site dilution and bond randomness. On the other hand, the thermal Hall conductivity is affected by these disorders differently. We find that the quantization of the thermal Hall conductivity is robust against the bond randomness but is fragile for the site dilution.

References

- [1] J. Nasu and Y. Motome: Phys. Rev. B **102** (2020) 054437.

Effect of quenched disorder on a triangular lattice fermionic model

Chisa HOTTA

Department of Basic Science,

The University of Tokyo, Meguro-ku Komaba, Tokyo 153-8902

We studied the fermionic model on a triangular lattice with quenched disorder[1]. We are targeting the so-called tV model on a triangular lattice consisting of transfer integrals t and nearest neighbor Coulomb repulsions V , whose ground state is known to host a Pinball liquid phase [2,3] at large V/t , which is a state where part of the fermions localize on one of the three-sublattices, and form a symmetry breaking long range order. The rest of the fermions remain metallic and propagate along $2/3$ of the lattice sites forming a honeycomb band. To be precise, the long range ordered fermions (pin) and metallic fermions(ball) are not fully separate, but exchange by the quantum fluctuation. In this study, we focus on the finite temperature properties of this phase, by adding a quenched disorder to the transfer integral.

However, it is quite difficult to fully solve the standard tV model at finite temperature in a reasonably large system size. Therefore, we introduce the Falikov-Kimball type of approximation and set the pins to be classical, while keep the balls to be quantum, and perform the Monte Carlo calculation. By changing the ratio of pin and ball and by

moving the location of pins, and each time diagonalizing the ball-fermions under the interaction from pins, the system is safely thermalized to the pinball-liquid phase. We made full use of the ISSP supercomputing system to perform the calculation up to the system size of 24×24 ; the finite temperature phase transition is observed as a divergence in the specific heat. Also the low energy profile of the pinball liquid state is well reproduced. We also found that at extremely low temperature, the introduction of the quenched disorder will drive the system to some sort of a glassy phase, where there starts to appear a domain wall structure of pinball phase. This domain becomes distinct as the system size becomes larger and the degree of disorder is increased, which is detected in the broad structure of the Replica overlap distribution function.

References

- [1] Keita Urakami and Chisa Hotta, in preparation.
- [2] Chisa Hotta and Nobuo Furukawa, Phys. Rev. B **74**, (2006)193107.
- [3] Chisa Hotta, Nobuo Furukawa, Akihiko Nakagawa, and Kenn Kubo, J. Phys. Soc. Jpn. **75**, (2006) 123704.

Ordered states in strongly correlated Dirac electron systems of organic conductors

Akito KOBAYASHI

*Department of Physics, Nagoya University
Nagoya 464-8602*

In the low temperature phase ($T < T_{co} = 135K$) of the organic Dirac electron system α -(BEDT-TTF) $_2$ I $_3$, it is believed that the electron correlation breaks the spatial inversion symmetry and transitions to a stripe charge ordered insulator. The electron correlation induces the reshaping of Dirac cones and the anomalous spin fluctuation. We investigated the electron correlation effects on the anomalous thermoelectric effects and the spin fluctuations[2, 4, 6]. In contrast, the element-substituted α -(BETS) $_2$ I $_3$ shows insulating behavior at low temperatures below 50 K, but no crystal symmetry breaking or charge density change is observed in X-rays, and no sign of magnetic transition is obtained from NMR. In this study, we constructed an extended Hubbard model based on first-principles calculations and analyzed it using mean-field approximation. It was shown that a magnetic transition occurs due to a short-range Coulomb interaction as shown in Fig. 1[3]. However, since no magnetic transition was observed in the experiment, it is necessary to investigate other possibilities. In addition, we showed possible edge magnetism in Dirac nodal line systems of single component molecular conductors [1, 5].

References

- [1] T. Kawamura, B. Zhou, Akiko Kobayashi, Akito Kobayashi, accepted to J. Phys. Soc. Jpn. (2021/03/30)

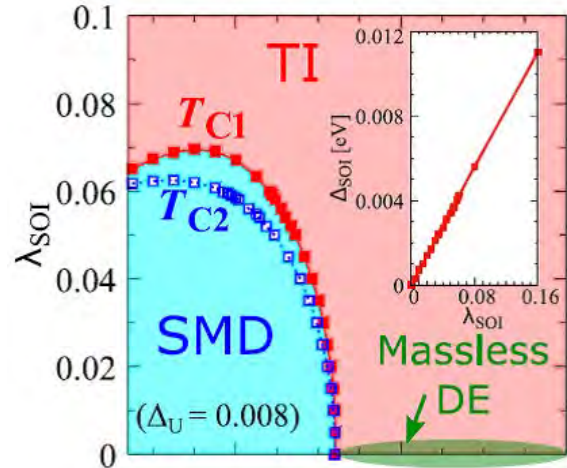


Figure 1: A candidate of ordered states in α -(BETS) $_2$ I $_3$.

- [2] M. Hirata, A. Kobayashi, C. Berthier and K. Kanoda, Rep. Prog. Phys. **84** 036502 (2021)
- [3] D. Ohki, K. Yoshimi, and A. Kobayashi, Phys. Rev. B **102**, 235116 (2020)
- [4] D. Ohki, M. Hirata, T. Tani, Kazushi K., and A. Kobayashi, Phys. Rev. Research **2**, 033479 (2020)
- [5] T. Kawamura, D. Ohki, B. Zhou, Akiko Kobayashi, Akito Kobayashi, J. Phys. Soc. Jpn. **89**, 074704 (2020)
- [6] D. Ohki, Y. Omori, A. Kobayashi, Phys. Rev. B **101**, 245201 (2020)

Development of electronic structure calculation for solids with post-Hartree-Fock calculations

Kazutaka NISHIGUCHI

Department of Physics, Osaka University

Toyonaka, Osaka 560-0043, Japan

– *Electronic structure calculation for solids with post-Hartree-Fock calculations* –

Continuing from our preceding-term study, we have theoretically studied a new method of electronic structure calculation for solids with quantum chemistry calculations. Our proposed procedure is as follows. We first start with Hartree Fock (HF) calculation for solids and construct maximally localized Wannier functions as a localized basis set. Then we consider a real-space cluster in the Wannier representation and solve it numerically with equation-of-motion coupled cluster (EOM-CC) theory. Here we have used VASP (The Vienna Ab initio Simulation Package) [1, 2, 3, 4, 5] in the HF calculations, Wannier90 [6, 7, 8, 9] in the wannierization method, and GELLAN program [10] in the EOM-CC calculations.

We apply this method to typical semiconductors, namely, bulk Si and SrTiO₃, and evaluate these energy band gaps as a benchmark. Developing the preceding-term study, we use symmetry-adapted Wannier functions [9] in constructing the localized basis set with Wannier90. We then can observe that the localized basis set can be obtained stably and the band gap can be improved compared to that with the HF calculations. However, it is still insufficient because the number of the localized bases is not sufficient to take into account the electron correlations. To increase the number of the localized bases will be an interesting future work.

– *Formation energy of n-type doping in*

CaZn₂X₂ (X = Sb, As, P) –

Continuing from our preceding-term study, we have numerically evaluated a formation energy of n-type doping in a strong candidate of high performance thermoelectric materials CaZn₂X₂ (X = Sb, As, P) by the first-principles calculations based on the density functional theory (DFT). We consider the chemical doping into the interstitial site and the element substitution of Ca, where the dopant is assumed to be the alkaline earth metals (Mg, Ca, Sr, Ba) and group 3 elements (Sc, Y, La). The ionization energy of these elements is relatively small as cations so that the smaller formation energy is expected. To take into account the chemical doping, the 3 × 3 × 2 supercell calculations are performed (Figure 1) with the Perdew Burke Ernzerhof (PBE) functional, namely, the generalized gradient approximation (GGA). Here we have used VASP [1, 2, 3, 4, 5] in the first-principles calculations.

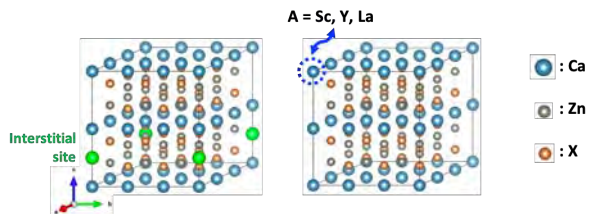


Figure 1: 3 × 3 × 2 supercell of CaZn₂X₂ (X = Sb, As, P). (Left) Doping into the interstitial site. (Right) Element substitution of Ca.

For the interstitial doping one can observe

in Figure 2 that the chemical doping of Ca and group 3 elements is favorable according to the formation energy. In addition, for the element substitution of Zn one can also see in Figure 3 that the element substitution for Sc is stable. This tendency of the formation energy is considered to depend on the ionization energy of these doping elements and the ionic radius against the interstitial site and Ca vacancy site. The improvement of the exchange correlation functional such as the hybrid functional and the inclusion of the finite-size supercell effect will be important future works.

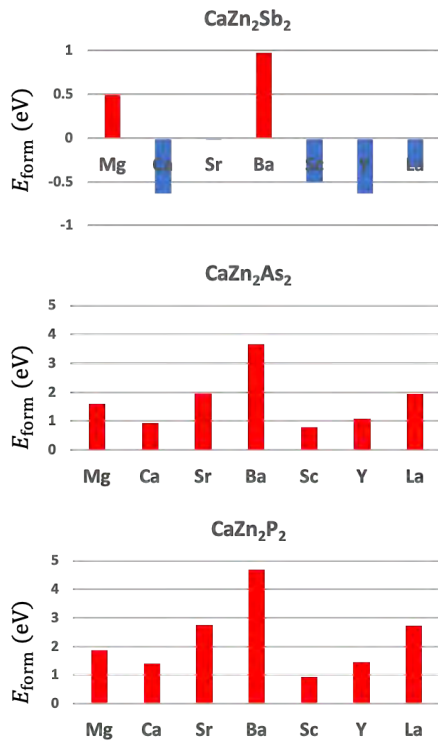


Figure 2: Formation energy of the doping into the interstitial site.

References

- [1] G. Kresse and J. Hafner, Phys. Rev. B **47** 558(R) (1993).
- [2] G. Kresse and J. Hafner, Phys. Rev. B **49** 14251 (1994).

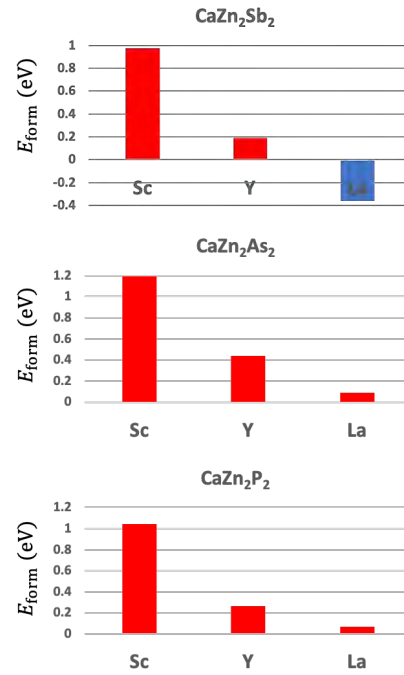


Figure 3: Formation energy of the element substitution of Ca.

- [3] G. Kresse and J. Furthmüller, Comput. Mater. Sci. **6** 15 (1996).
- [4] G. Kresse and J. Furthmüller, Phys. Rev. B **54** 11169 (1996).
- [5] VASP (The Vienna Ab initio Simulation Package): <https://www.vasp.at>
- [6] N. Marzani and D. Vanderbilt, Phys. Rev. B **56** 12847 (1997).
- [7] I. Souza, N. Marzani, and D. Vanderbilt, Phys. Rev. B **65** 035109 (2001).
- [8] Wannier90: <http://www.wannier.org>
- [9] R. Sakuma, Phys. Rev. B **87** 235109 (2013).
- [10] GELLAN: A hierarchical massively-parallel quantum chemistry program, Kobe University

Development of electronic structure calculation for solids with quantum chemistry calculations

Kazutaka NISHIGUCHI

Department of Physics, Osaka University

Toyonaka, Osaka 560-0043, Japan

– *Electronic structure calculation for solids with quantum chemistry calculations* –

A new method of electronic structure calculation for solids with quantum chemistry calculations have been studied theoretically. We first start with Hartree Fock (HF) calculation for solids and construct maximally localized Wannier functions as a localized basis set. Then we consider a real-space cluster in the Wannier representation and solve it numerically with equation-of-motion coupled cluster (EOM-CC) theory. Here we have used VASP (The Vienna Ab initio Simulation Package) [1, 2, 3, 4, 5] in the HF calculations, Wannier90 [6, 7, 8] in the wannierization method, and GELLAN program [9] in the EOM-CC calculations.

We apply this method to typical semiconductors, namely, bulk Si and SrTiO₃, and evaluate these energy band gaps as a benchmark. We can observe that the band gap can be improved compared to that with the HF calculations, but it is not sufficient because the localized basis set is difficult to converge stably. To achieve stable construction of the localized basis set will be an interesting future work.

– *Formation energy of n-type doping in CaZn₂Sb₂* –

A formation energy of n-type doping in a strong candidate of high performance thermoelectric materials CaZn₂Sb₂ have been numerically evaluated by the first-principles calculations based on the density functional theory (DFT). We consider the chemical doping into the interstitial site and the element substitu-

tion of Zn, where the dopant is assumed to be the alkaline earth metals (Mg, Ca, Sr, Ba) and group 3 elements (Sc, Y, La). The ionization energy of these elements is relatively small as cations, so that the smaller formation energy is expected. To take into account the chemical doping, the $3 \times 3 \times 2$ supercell calculations are performed (Figure 1) with the Perdew Burke Ernzerhof (PBE) functional, namely, the generalized gradient approximation (GGA). Here we have used VASP [1, 2, 3, 4, 5] in the first-principles calculations.

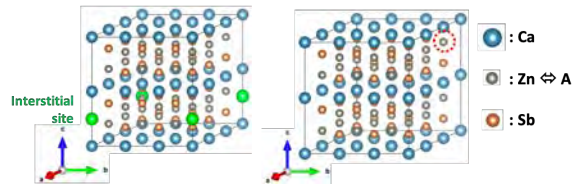


Figure 1: $3 \times 3 \times 2$ supercell of CaZn₂Sb₂. (Left) Doping into the interstitial site. (Right) Element substitution of Zn.

For the interstitial doping one can observe in Figure 2 that the chemical doping of Ca and group 3 elements is favorable according to the formation energy. In addition, for the element substitution of Zn one can also see in Figure 3 that the element substitution for Mg, Ca, Sr, and group 3 elements is stable. This tendency of the formation energy is considered to depend on the ionization energy of these doping elements and the ionic radius against the interstitial site and Zn vacancy site. On the other hand, the calculated formation energy is

now understood to be qualitative because the PBE functional is not sufficient to evaluate the accurate energy band gap for semiconductors and the finite-size supercell effect is not included in these calculations, but the tendency of the formation energy is important for material synthesis of n-type semiconductors. The improvement of the exchange correlation functional such as the hybrid functional and the inclusion of the finite-size supercell effect will be important future works.

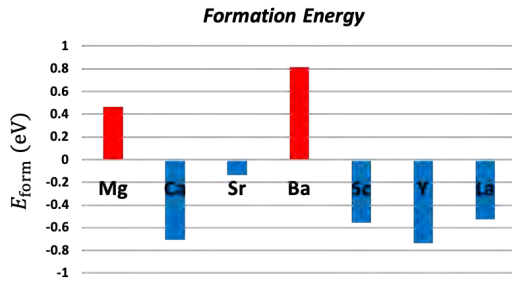


Figure 2: Formation energy of the doping into the interstitial site.

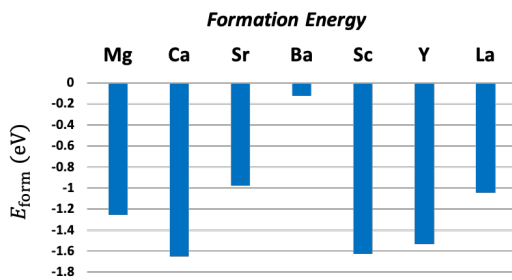


Figure 3: Formation energy of the element substitution of Zn.

References

- [1] G. Kresse and J. Hafner, Phys. Rev. B **47** 558(R) (1993).
- [2] G. Kresse and J. Hafner, Phys. Rev. B **49** 14251 (1994).
- [3] G. Kresse and J. Furthmüller, Comput. Mater. Sci. **6** 15 (1996).
- [4] G. Kresse and J. Furthmüller, Phys. Rev. B **54** 11169 (1996).
- [5] VASP (The Vienna Ab initio Simulation Package): <https://www.vasp.at>
- [6] N. Marzani and D. Vanderbilt, Phys. Rev. B **56** 12847 (1997).
- [7] I. Souza, N. Marzani, and D. Vanderbilt, Phys. Rev. B **65** 035109 (2001).
- [8] Wannier90: <http://www.wannier.org>
- [9] GELLAN: A hierarchical massively-parallel quantum chemistry program, Kobe University

Quantum Monte Carlo simulation and electronic state calculations in correlated electron systems

Takashi YANAGISAWA

Electronics and Photonics Research Institute

National Institute of Advanced Industrial Science and Technology (AIST)

AIST Central 2, 1-1-1 Umezono, Tsukuba 305-8568

We carried out numerical calculations on the basis of the optimized variational Monte Carlo method[1, 2, 3, 4]. We have investigated the ground-state phase diagram of the two-dimensional Hubbard model and the two-dimensional d-p model. We performed parallel computations by using a Monte Carlo algorithm. In order to reduce statistical errors, we carried out 200 ~ 500 parallel calculations. Parallel computing is very necessary to reduce Monte Carlo statistical errors.

We employed the improved wave function of an $\exp(-\lambda K) - P_G$ -type[1]. This wave function is a very good many-body wave function because the ground-state energy is lowered greatly and the ground-state energy is lower than those that are evaluated by any other wave functions[2]. We can improve the wave function systematically by multiplying by operators P_G and $e^{-\lambda K}$ several times.

We exhibit the condensation energy as a function of the doping rate x for the three-band d-p model in Fig. 1 where $U_d = 10t_{dp}$ and the level difference is taken as $\Delta_{dp} \equiv \epsilon_p - \epsilon_d = t_{dp}$ [6]. There is the AF region when x is small and the SC region exists near the optimum region $x \sim 0.2$. We should mention that there is a phase-separated region in the low-doping region where $x < 0.07$. This indicates the existence of AF insulator phase in the low doping region. This is similar to the phase diagram of the 2D Hubbard model. The phase separation (PS) is, however, dependent on the level difference Δ_{dp} . As Δ_{dp} decreases, the phase-separated region decreases and vanishes when Δ_{dp} approaches zero. Thus the area of phase-separated region can be controlled by changing

the band parameters.

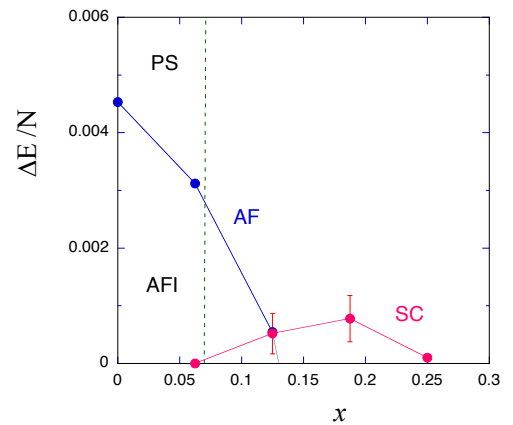


Figure 1: AF and SC condensation energies as a function of the hole doping rate x for $\Delta_{dp} = 1$ on a 8×8 lattice with $t_{pp} = 0.4$ and $U_d = 10$ in units of t_{dp} . There is a phase-separated region when x is small.

References

- [1] T. Yanagisawa et al., J. Phys. Soc. Jpn. 67, 3867 (1998).
- [2] T. Yanagisawa, J. Phys. Soc. Jpn. 85, 114707 (2016).
- [3] T. Yanagisawa, J. Phys. Soc. Jpn. 88, 054702 (2019).
- [4] T. Yanagisawa, Condensed Matter 4, 57 (2019).
- [5] T. Yanagisawa, Phys. Lett. A403, 127382 (2021).
- [6] T. Yanagisawa et al., EPL (2021).

Calculation of the electronic state in a large model of the organic charge ordering system using mVMC

Masatoshi SAKAI, Riku TAKEDA, Ryoma ISHII

*Department of Electrical and Electronic Engineering,
Chiba University, 1-33 Yayoi-cho Inage, Chiba 263-8522*

We have studied the electronic state of the large-size model of the organic charge order system by using the supercomputer. We made a base model of α -(BEDT-TTF)₂I₃ by citing reference [1] and carried out a 28 x 28 site calculation to reveal the electron number dependence of the charge order structure of the correlated electron system. The simulation software mainly used in this work was mVMC, as preinstalled in the ENAGA and OHTAKA supercomputer systems. The electron number dependence of the charge order structure is significant for us to support our experimental work. Our experimental work was the metal-insulator phase transition transistor which was observed in organic charge order material of α -(BEDT-TTF)₂I₃ near the metal-insulator phase transition at 137 K. We expect that the calculation of electron number dependence of charge order structure and energy will give a theoretical backbone to our experimental result. Our group made an effort to learn about supercomputer and mVMC, and now we are finally in routine calculation by varying electron number from 376 to 404 electrons in

the system.

The other work in progress is about β -(BEDT-TTF)₂PF₆, of which metal-insulator phase transition is 297 K [2]. In this work, we could not find the physical parameters in previous works, so we began to calculate from the band structure before carrying out model calculation of correlated electronic system. We used Quantum Espresso and Respack to obtain physical parameters to build the calculation model used in mVMC or HPhi. We learned Quantum Espresso and Respack, and now we have just achieved the end of the calculation of the Respack. Therefore, we will verify the results and apply the next step by using mVMC or HPhi to reveal the physical principle of the phase transition field-effect transistor.

References

- [1] Daigo Ohki, Genki Matsuno, Yukiko Omori and Akito Kobayashi: Crystals 8, (2018) 137.
- [2] Hayao Kobayashi, Takehiko Mori, Reizo Kato, Akiko Kobayashi, Yukiyoishi Sasaki, Gunzi Saito and Hiroo Inokuchi: Chem. Lett. (1983) 581.

Study for high- T_c cuprates using four-band d - p model

Hiroshi WATANABE

*Research Organization of Science and Technology, Ritsumeikan University
1-1-1 Noji-Higashi, Kusatsu-shi, Shiga 525-8577*

The discovery of superconductivity in cuprates [1] has brought about the significant progress in strongly-correlated electron systems. However, we have not yet reached a unified understanding of their properties, including their material dependence of the superconducting transition temperature T_c . Recent development of theories and experiments sheds light on the importance of the orbital degree of freedom in cuprates [2, 3]. To elucidate the material dependence of T_c , we study the four-band d - p model for La_2CuO_4 and $\text{HgBa}_2\text{CuO}_4$ systems that properly includes the orbital degree of freedom. The ground state properties are studied with the variational Monte Carlo (VMC) method. The Gutzwiller-Jastrow type wave function is used for the VMC trial wave function. The system size for the calculation is $N=24\times 24=576$ unit cells (and thus $576\times 4=2304$ orbitals in total), which is large enough to avoid finite size effects.

The superconducting correlation function P^{dd} vs hole doping rate δ for the La_2CuO_4 and $\text{HgBa}_2\text{CuO}_4$ systems are shown in Fig. 1. The dome-shaped behavior and the material dependence are consistent with experiments. We show that the Cu d_{z^2} orbital contribution around the Fermi energy is destructive for d -wave superconductivity, and thereby becomes a key factor to determine T_c . The energy difference Δ_{dp} between Cu $d_{x^2-y^2}$ and O p orbitals is also shown to be a key factor. Our result accounts for the empirical correlation between T_c and model parameters and gives the unified description beyond the usual one-band Hubbard, t - J , and even three-band d - p models.

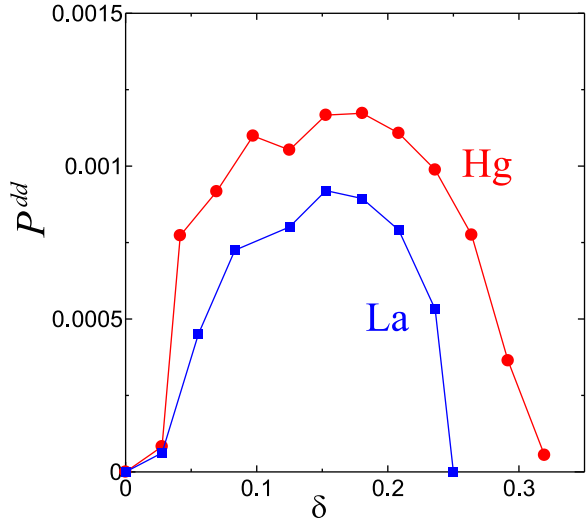


Figure 1: Superconducting correlation function P^{dd} vs hole doping rate δ for the La_2CuO_4 and $\text{HgBa}_2\text{CuO}_4$ systems.

References

- [1] J. G. Bednorz and K. A. Müller, *Z. Phys. B* **64**, 189 (1986).
- [2] H. Sakakibara et al., *Phys. Rev. Lett.* **105**, 057003 (2010).
- [3] C. E. Matt et al., *Nat. Commun.* **9**, 972 (2018).

Studies of the superconductivity and magnetic states in the strongly correlated electron systems using Hubbard models.

Atsushi Yamada

*Department of Physics, Chiba University
Chiba 263-8522, Japana, Chiba 277-8581*

A spin liquid state has attracted a lot of interest. This state is realized in geometrically frustrated systems like the charge organic transfer salts κ -(BEDT-TTF)₂X[1] and Cs₂CuCl₄. [2] Hubbard model on the anisotropic triangular lattice is a simple theoretical model of these compounds, and spin liquid state is found in this model. [3] A spin liquid could arise also in the intermediate coupling region of strongly correlated systems between a semi-metal and ordered state, because in this case a correlation-driven insulating gap might open before the system becomes ordered. This possibility might be realized in the half-filled Hubbard model on the honeycomb lattice, where a semi-metal is realized at $U = 0$.

We have studied the magnetic and metal-to-insulator transitions by variational cluster approximation using 10-site and 16-site clusters as a reference system. Parts of numerical calculations were done using the computer facilities of the ISSP. We found that $U_{AF} = 2.7$ and $U_{MI} = 3.0$ for 10-site cluster, and $U_{AF} = 2.7$ and $U_{MI} = 3.2$ for 16-site cluster. [5] This result also rules out the existence of the spin liquid in this model. Our results agree with recent large scale Quantum Monte Carlo simulations. [4]

We are currently improving our program using MPI technique so that we will be able to study a larger cluster size system.

References

- [1] Y. Shimizu, K. Miyagawa, K. Kanoda, M. Maesato, and G. Saito, Phys. Rev. Lett. **91**, 107001 (2003); Y. Kurosaki, Y. Shimizu, K. Miyagawa, K. Kanoda, and G. Saito, Phys. Rev. Lett. **95**, 177001 (2005).
- [2] R. Coldea, D.A. Tennant, A.M. Tsvelik, and Z. Tylczynski, Phys. Rev. Lett. **86**, 1335 (2001); R. Coldea, D.A. Tennant, and Z. Tylczynski, Phys. Rev. Lett. **68**, 134424 (2003).
- [3] T. Yoshioka, A. Koga, and N. Kawakami, Phys. Rev. Lett. **103**, 036401 (2009); P. Sahebsara and D. Sénéchal, Phys. Rev. Lett. **100**, 136402 (2008); L.F. Tocchio, H. Feldner, F. Becca, R. Valentí, and C. Gros, Phys. Rev. B **87**, 035143 (2013); A. Yamada, Phys. Rev. B **89**, 195108 (2014); L.F. Tocchio, C. Gros, R. Valentí, F. Becca, Phys. Rev. B **89**, 235107 (2014); A. Yamada, Phys. Rev. B **90**, 235138 (2014).
- [4] S. Sorella, Y. Otsuka, and S. Yunoki, Sci. Rep. **2**, 992 (2012); F. F. Assaad and I. F. Herbut, Phys. Rev. X **3**, 031010 (2013); F. Parisen Toldin, M. Hohenadler, F. F. Assaad, and I. F. Herbut, Phys. Rev. B **91**, 165108 (2015).
- [5] A. Yamada, Int. J. Mod. Phys. B **30**, 1650158 (2016).